

# Automatic arrhythmia detection based on time and time–frequency analysis of heart rate variability

Markos G. Tsipouras, Dimitrios I. Fotiadis\*

*Unit of Medical Technology and Intelligent Information Systems, Department of Computer Science, University of Ioannina, GR 45110, Ioannina, Greece*

Received 2 August 2002; received in revised form 27 January 2003; accepted 11 February 2003

## KEYWORDS

Arrhythmia detection;  
Heart rate variability;  
Time–frequency  
analysis

**Summary** We have developed an automatic arrhythmia detection system, which is based on heart rate features only. Initially, the RR interval duration signal is extracted from ECG recordings and segmented into small intervals. The analysis is based on both time and time–frequency ( $t-f$ ) features. Time domain measurements are extracted and several combinations between the obtained features are used for the training of a set of neural networks. Short time Fourier transform and several time–frequency distributions (TFD) are used in the  $t-f$  analysis. The features obtained are used for the training of a set of neural networks, one for each distribution. The proposed approach is tested using the MIT-BIH arrhythmia database and satisfactory results are obtained for both sensitivity and specificity (87.5 and 89.5%, respectively, for time domain analysis and 90 and 93%, respectively, for  $t-f$  domain analysis).

© 2003 Elsevier Ireland Ltd. All rights reserved.

## 1. Introduction

Arrhythmia is a collective term for any cardiac rhythm that deviates from normal sinus rhythm. Arrhythmia may be due to a disturbance in impulse formation or conduction, or both, but it is not always an irregular heart activity [1]. Respiratory sinus arrhythmia is a natural periodic variation in RR-intervals, corresponding to respiratory activity. Impulse formation may be sinus or ectopic, the rhythm regular or irregular and the heart rate fast, normal or slow [2,3]. Therefore, the detection of abnormal cardiac rhythms and automatic discrimination from the normal heart activity became an

important task for clinical reasons. Most of the studies address the detection and identification of life threatening arrhythmias and specifically ventricular and atrial fibrillation and ventricular tachycardia. Various detection algorithms have been proposed, such as the sequential hypothesis testing [4], the multiway sequential hypothesis testing [5], the threshold-crossing intervals [6], the auto-correlation function [6], the VF-filter [6] and algorithms based on neural-networks [7–9]. Time–frequency ( $t-f$ ) analysis [10] and wavelet analysis [11,12] have also been used. Recent approaches utilize complexity measure [13] and multifractal analysis combined with a fuzzy Kohonen neural network [14].

Heart rate variability (HRV) refers to the beat-to-beat heart rate alterations. HRV believed to be a good marker of the individual's health condition and heart diseases [15]. Therefore, HRV

\*Corresponding author. Tel.: +30-6510-98803;  
fax: +30-6510-97099.

E-mail addresses: markos@cs.uoi.gr (M.G. Tsipouras),  
fotiadis@cs.uoi.gr (D.I. Fotiadis).

analysis became a critical tool in cardiology for the diagnosis of heart diseases. Time domain analysis of RR-intervals includes calculation of several common statistical indices [16,17] and graphical representation of the RR-interval duration signal [18,19]. Frequency analysis provides the power spectrum density (PSD) of the RR-interval duration signal using Fourier transform and autoregressive techniques [20–25].  $t-f$  analysis is based on the use of short time Fourier transform (STFT), time–frequency distributions (TFDs) and wavelet analysis [10–12] of the RR-interval duration signal. Other approaches for the HRV analysis include methods from nonlinear mathematics and chaos theory, such as fractal [26,27] and approximate entropy [27] analysis.

More specifically in the  $t-f$  analysis Wigner-Ville (WV) distribution [28,29] and improved forms of WV, such as pseudo Wigner-Ville (PWV) [30–33] and smoothed pseudo Wigner-Ville (SPWV) [34–36], discrete Fourier transform and selective discrete Fourier transform [37–40], cone shaped kernel distribution [10], Choi-Williams distribution [41] and other exponential distributions [42] have been used.

In this paper we explore time and  $t-f$  analysis of the RR-interval duration signal in order to detect arrhythmic segments in ECGs [43]. Selected features from the time domain and  $t-f$  analysis are

extracted. Several combinations of those features are used for training a set of neural networks. The decision is finally obtained using decision rules.

## 2. Materials and methods

Our analysis is carried out in four stages. First a preprocessing procedure is used to extract the tachograms from the ECGs. The tachograms are segmented into small segments. Each segment contains 32 RR-intervals. In the second stage time domain or  $t-f$  methods are applied to extract the corresponding features. In the third stage the extracted features are used for training a set of neural networks. In the fourth stage detection of arrhythmic segments is carried out using decision rules which are fed with the outputs of the neural networks.

### 2.1. Preprocessing

Preprocessing is carried out in two steps. In the first step we extract the tachograms from the ECG recordings. The dataset used in our study is the MIT-BIH arrhythmia database [44,45]. This database consists of 48 ECG recordings. The length of each recording is 30 min, which results to a

**Table 1** Beat annotations of the MIT-BIH arrhythmia database

| Annotation symbol | Meaning                                   | Classification in our case |
|-------------------|---|----------------------------|
| N                 | Normal beat                               | Normal                     |
| L <sup>a</sup>    | Left bundle branch block beat             | Normal                     |
| R <sup>a</sup>    | Right bundle branch block beat            | Normal                     |
| A                 | Atrial premature beat                     | Arrhythmic                 |
| a                 | Aberrated atrial premature beat           | Arrhythmic                 |
| J                 | Nodal (junctional) premature beat         | Arrhythmic                 |
| S                 | Supraventricular premature beat           | Arrhythmic                 |
| V                 | Premature ventricular contraction         | Arrhythmic                 |
| F                 | Fusion of ventricular and normal beat     | Arrhythmic                 |
| [                 | Start of ventricular flutter/fibrillation | Arrhythmic                 |
| !                 | Ventricular flutter wave                  | Arrhythmic                 |
| ]                 | End of ventricular flutter/fibrillation   | Arrhythmic                 |
| e                 | Atrial escape beat                        | Arrhythmic                 |
| j                 | Nodal (junctional) escape beat            | Arrhythmic                 |
| n                 | Supraventricular escape beat              | Arrhythmic                 |
| E                 | Ventricular escape beat                   | Arrhythmic                 |
| P <sup>b</sup>    | Paced beat                                | Normal                     |
| f <sup>b</sup>    | Fusion of paced and normal beat           | Normal                     |
| p                 | Non-conducted P-wave (blocked APB)        | Normal                     |
| Q                 | Unclassifiable beat                       | Normal                     |
|                   | Isolated QRS-like artifact                | Normal                     |

<sup>a</sup> L and R annotated beats are classified as “Normal” because they cannot be detected as arrhythmic using only heart rate and HRV.

<sup>b</sup> Beats with annotations P and f are considered as normal because pace is not in the interest of this study.

total of 24 h of recordings with 112 568 RR-intervals. All RR-intervals are used except for those close to the start or end of each recording, which are excluded during segmentation. Each beat in the database is annotated with a character annotation (Table 1). The RDNN software, which accompanies the MIT-BIH database, is used for QRS detection. Then the RR-interval duration signal (tachogram) can be obtained.

In the second step the tachograms are cut into small segments of 32 RR-intervals each, and each segment is characterized as normal or arrhythmic using the MIT-BIH beat annotation. This results to 3456 segments. For each RR-interval the characterization of the second beat is used for its characterization. The characterization of the MIT-BIH arrhythmia database beats as “normal” or “arrhythmic” is shown in Table 1. A 32 RR-interval segment is characterized as “normal” if it contains more than 30 “normal” RR-intervals otherwise is characterized as “arrhythmic”.

## 2.2. Time domain analysis

We apply time domain analysis on the segmented dataset. Time domain analysis results in indices and markers obtained from the tachogram, such as mean and standard deviation of RR-intervals, mean and standard deviation of differences between adjacent RR-intervals, difference between the longer and the shorter RR-interval and others. The standard deviation of all normal-to-normal RR-intervals (SDRR) is the simplest feature that can be extracted from the tachogram. The root mean square of successive differences of all normal-to-normal RR-intervals ( $r\_MSSD$ ) and the standard deviation of successive differences of all normal-to-normal RR-intervals (SDSD) are also widely used

indices. The percentage of intervals presenting time duration difference between adjacent normal-to-normal RR-intervals greater than 50 ms (pNN50) is another HRV characteristic. In many studies this percentage is used with different time threshold, such as 5 ms (pNN5) or 10 ms (pNN10) [16,17].

We use all possible combinations among the above mentioned time analysis features (each combination contains one, two, three, four, five or six features) to create the pattern set for the classification stage. This leads to a total of 63 feature combinations, which are shown in Table 2, with 3426 patterns each. In the third stage (classification stage) we train a feed-forward back-propagation neural network, for each feature combination. We use 1426 patterns randomly chosen from the total of 3426 patterns as training set. Several neural network architectures have been tested and we have chosen the one that performs better:  $N$  inputs (number of features used in the specific combination), one hidden layer with 20 neurons and one output, being a real number between 0 and 1. The final “normal” or “arrhythmic” classification is made with 0.5 threshold on the networks’ output. The training of the neural network ends when the square error is less than 0.01 or the training epochs are more than 2000. Finally, we result in a set with 63 neural networks (one for each combination). The outputs of the neural networks are fed into a set of decision rules as it is described below (forth stage).

## 2.3. Time–frequency analysis

STFT and various TFDs are used for the  $t - f$  analysis of the segmented dataset. For STFT, the signal  $x(u)$  is pre-windowed around a time instant  $t$ , and the Fourier Transform is calculated for each time

**Table 2** Combinations of time domain features

|     | Feature combination | Features                                   |
|-----|---------------------|--|
| 1   | 1                   | SDNN                                       |
| 2   | 2                   | $r\_MSSD$                                  |
| 3   | 12                  | SDNN, $r\_MSSD$                            |
| 4   | 3                   | SDSD                                       |
| 5   | 13                  | SDNN, SDSD                                 |
| 6   | 23                  | SDNN, $r\_MSSD$                            |
| 7   | 123                 | SDNN, $r\_MSSD$ , SDSD                     |
| 8   | 4                   | pNN5                                       |
| ... | ...                 | ...  |
| 60  | 3456                | SDSD, pNN5, pNN10, pNN50                   |
| 61  | 13456               | SDNN, SDSD, pNN5, pNN10, pNN50             |
| 62  | 23456               | $r\_MSSD$ , SDSD, pNN5, pNN10, pNN50       |
| 63  | 123456              | SDNN, $r\_MSSD$ , SDSD, pNN5, pNN10, pNN50 |

instant  $t$ .

$$\text{STFT}(t, f) = \int_{-\infty}^{+\infty} x(\tau)h(\tau - t)e^{-if\tau}d\tau \quad (1)$$

where  $h(t)$  is a short time window, localized around  $t=0$  and  $f=0$ . STFT suffers of trade-off between its window length and its frequency resolution. The TFDs used in our study belong to the Cohen's class of distributions [46] and are given by the following formula:

$$\rho(t, f) = \int \int \int e^{i2\pi v(u-t)} g(v, \tau) x^* \left( u - \frac{1}{2}\tau \right) x \left( u + \frac{1}{2}\tau \right) e^{-i2\pi f\tau} dv d\tau \quad (2)$$

where  $x^*(t)$  is the complex conjugate of the signal and  $g(v, \tau)$  is an arbitrary function called kernel. The kernel is different for each TFD. Table 3 shows selected TFDs, which are used in our study and the corresponding kernels [46–55].

For each 32 RR-interval segment STFT and all TFDs are applied (totally 19 methods) and the PSD is computed (Fig. 1). For STFT a Hamming nine-point length window is used. All TFDs, except Margenau-Hill, Page, Rihaczek and Wigner-Ville, use frequency and/or time smoothing windows, which were set as Hamming nine-point length windows. For the computation of the STFT and the TFDs for each segment we use the previous and the next segment to avoid problems in the margins of the segment. The PSD is computed and the amplitude is normalized in  $[-1, 1]$  interval. This represents the fractional energy of the signal in time  $t$  and frequency  $f$  (Fig. 1a). We obtain horizontal slices from the PSD for amplitude = 0.0, 0.2, 0.4, 0.6, 0.8 and 1.0, which contain the corresponding PSD trace (Fig. 1b). The areas between adjacent slide traces are calculated (Fig. 1c and d). These areas are the  $t - f$  features. Six features for each TFD are computed and they are used for the training of the neural networks (Fig. 2).

**Table 3** TFDs

|    | Distribution                             | Kernel ( $g(v, \tau)$ )   |   |
|----|--|---|---|
| 1  | Born-Jordan                              | $\frac{\sin(\pi v \tau)}{\pi v \tau}$   |   |
| 2  | Butterworth                              | $\frac{1}{1 + \left(\frac{v}{v_1}\right)^{2N} \left(\frac{\tau}{\tau_1}\right)^{2M}}$ | $N, M, v_1, \tau_1 > 0$                                 |
| 3  | Choi-Williams                            | $e^{-(\pi v \tau)^2 / 2\sigma^2}$   | $\sigma$ : scaling factor                               |
| 4  | Generalized rectangular                  | $\frac{\sin\left(\frac{2\pi\sigma v}{ \tau ^\alpha}\right)}{\pi v}$                   | $\sigma$ : scaling factor; $\alpha$ : dissymmetry ratio |
| 5  | Margenau-Hill                            | $\text{Cos}(\pi v \tau)$  |   |
| 6  | Pseudo Margenau-Hill                     | $h(\tau)\text{cos}(\pi v \tau)$   | $h(\tau)$ : window function                             |
| 7  | Margenau-Hill-spectrogram                | $h(\tau)\text{cos}(\pi v \tau)A_x^*(v, \tau)$   | $A_x(v, \tau)$ : ambiguity function                     |
| 8  | Page                                     | $e^{j\pi v  \tau }$   |   |
| 9  | Pseudo page                              | $h(\tau)e^{j\pi v  \tau }$  | $h(\tau)$ : window function                             |
| 10 | Wigner-Ville                             | 1   |   |
| 11 | PWV                                      | $h(\tau)$   | $h(\tau)$ : window function                             |
| 12 | Smoothed PWV                             | $G(v)h(\tau)$   | $h(\tau)$ : window function                             |
| 13 | Rihaczek                                 | $e^{j\pi v \tau}$   |   |
| 14 | Reduced interference (Bessel window)     | $\int_{-\infty}^{+\infty} h(t)e^{-j2\pi v \tau t} dt$                                 | $h(t)$ : Bessel window                                  |
| 15 | Reduced interference (Hanning window)    | $\int_{-\infty}^{+\infty} h(t)e^{-j2\pi v \tau t} dt$                                 | $h(t)$ : Hanning window                                 |
| 16 | Reduced interference (Binomial window)   | $\int_{-\infty}^{+\infty} h(t)e^{-j2\pi v \tau t} dt$                                 | $h(t)$ : binomial window                                |
| 17 | Reduced interference (Triangular window) | $\int_{-\infty}^{+\infty} h(t)e^{-j2\pi v \tau t} dt$                                 | $h(t)$ : triangular window                              |
| 18 | Zhao-Atlas-Marks                         | $h(\tau)\frac{\sin(\pi v \tau)}{\pi v \tau}$  | $h(\tau)$ : window function                             |

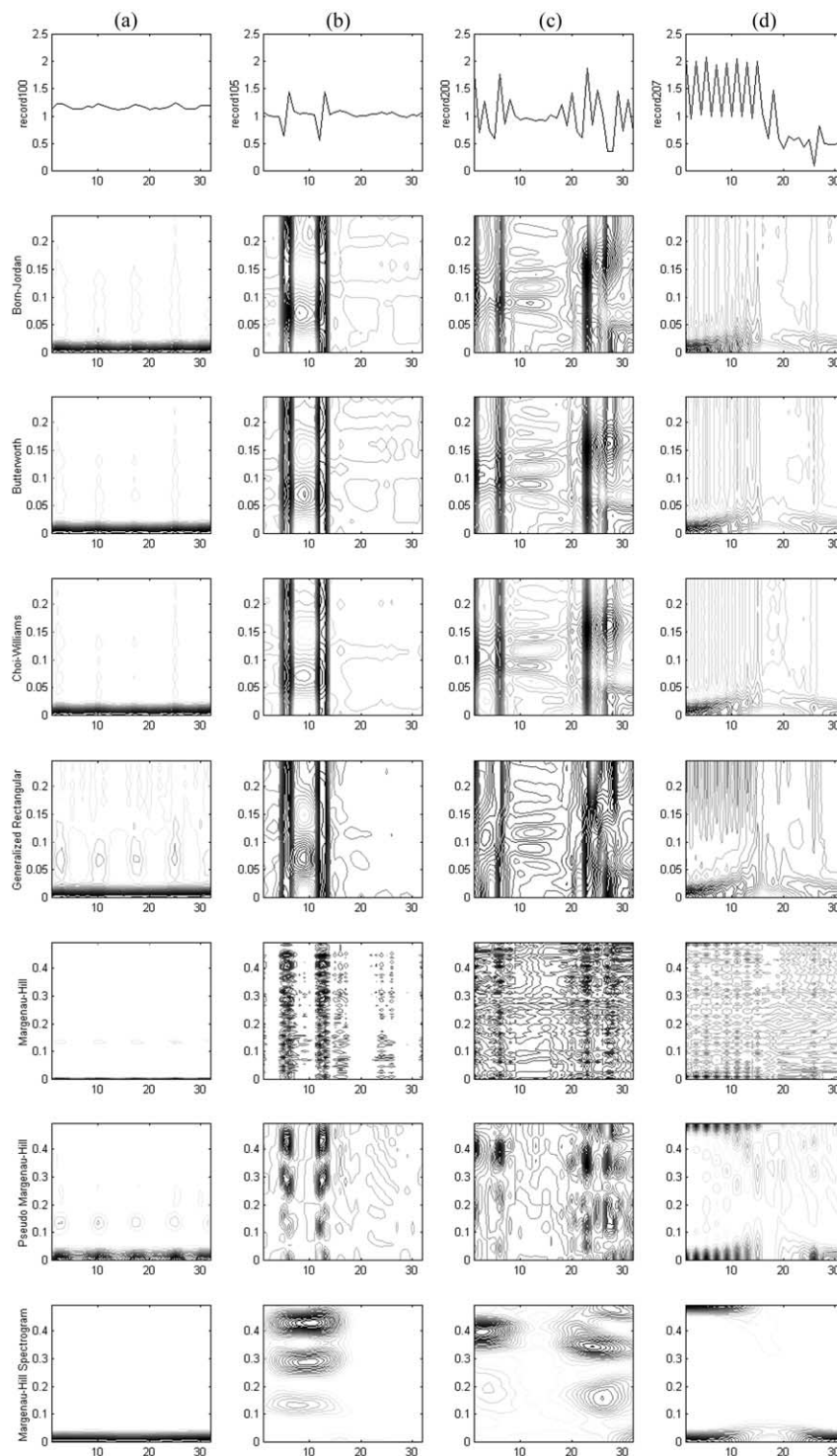


**Fig. 1** PSD for RR-interval segments containing: (a) normal sinus rhythm (from recording 100 of the MIT-BIH database); (b) normal sinus rhythm with two premature ventricular contractions (from recording 105 of the MIT-BIH database); (c) normal sinus rhythm mixed with premature ventricular contractions (from recording 200 of the MIT-BIH database); (d) rhythm consisting of premature ventricular contractions, left bundle branch block and right bundle branch block beats changing to premature ventricular contractions and then to ventricular flutter/fibrillation (from recording 207 of the MIT-BIH database).



# Explore Litigation Insights

Docket Alarm provides insights to develop a more informed litigation strategy and the peace of mind of knowing you're on top of things.

## Real-Time Litigation Alerts



Keep your litigation team up-to-date with **real-time alerts** and advanced team management tools built for the enterprise, all while greatly reducing PACER spend.

Our comprehensive service means we can handle Federal, State, and Administrative courts across the country.

## Advanced Docket Research



With over 230 million records, Docket Alarm's cloud-native docket research platform finds what other services can't. Coverage includes Federal, State, plus PTAB, TTAB, ITC and NLRB decisions, all in one place.

Identify arguments that have been successful in the past with full text, pinpoint searching. Link to case law cited within any court document via Fastcase.

## Analytics At Your Fingertips



Learn what happened the last time a particular judge, opposing counsel or company faced cases similar to yours.

Advanced out-of-the-box PTAB and TTAB analytics are always at your fingertips.

## API

Docket Alarm offers a powerful API (application programming interface) to developers that want to integrate case filings into their apps.

## LAW FIRMS

Build custom dashboards for your attorneys and clients with live data direct from the court.

Automate many repetitive legal tasks like conflict checks, document management, and marketing.

## FINANCIAL INSTITUTIONS

Litigation and bankruptcy checks for companies and debtors.

## E-DISCOVERY AND LEGAL VENDORS

Sync your system to PACER to automate legal marketing.